A Combined Experimental and Theoretical Study of Iron Dinitrogen Complexes: $Fe(N_2)$, $Fe(NN)_x$ ($x = 1-5$), and $Fe(NN)_3^-$

Zhang-Hui Lu,[†,‡] Ling Jiang,[†] and Qiang Xu*[,†,‡]

National Institute of Advanced Industrial Science and Technology (AIST), Ikeda, Osaka 563-8577, Japan, and Graduate School of Engineering, Kobe University, Nada Ku, Kobe, Hyogo 657-8501, Japan

Received: November 8, 2009; Revised Manuscript Received: December 28, 2009

Reactions of laser-ablated iron atoms with dinitrogen in excess neon produce the iron dinitrogen complexes $Fe(N_2)$, $Fe(NN)_x$ ($x = 1-5$), and $Fe(NN)_3^-$ through capture of the ablated electron. The reaction products are characterized on the basis of isotopic shifts, mixed isotopic splitting patterns, stepwise annealing, change of reagent concentration and laser energy, CCl_4-doping experiments, and comparison with theoretical predictions from density functional theory calculations. The overall agreement between the experimental and calculated vibrational frequencies, relative absorption intensities, and isotopic shifts supports the identification of these species from the matrix infrared spectra. Natural bond orbital analysis and reaction pathways for the formation of the products are discussed.

Introduction

Iron is a very important metal in many fields such as materials, chemistry, and biology. Especially, the interaction of iron with dinitrogen is of considerable practical and theoretical importance in the widely different fields of catalysis, biology, and atmospheric chemistry.[1] In catalysis, the dissociation of N_2 over Fe in the Haber process is critical in the production of NH_3,[2] and an iron dinitrogen intermediate has been suggested in the nitrogen fixation by the nitrogenase enzyme.[3] The long-standing goal of elucidating mechanisms of the reactions involving dinitrogen has motivated numerous experimental and theoretical investigations of the interactions between iron and dinitrogen.[4−17] Molecular adsorption of N_2 onto iron surfaces and clusters indicates that the dissociative chemisorption proceeds slowly and the adsorbed species has been proposed as an intermediate in the catalytic dissociation of N_2.[5−7] The reactions of Fe atoms with N_2 in low temperature matrices have been investigated, and the complicated IR spectra were attributed to several unsaturated iron nitride and iron dinitrogen complexes, among which some species were tentatively assigned.[9−13] These species are important models for understanding iron catalyst systems. The bonding nature of iron atoms with nitrogen has been reported by using the powerful technique of density functional theory or other theoretical methods.[14−18]

Previous studies have shown that, with the aid of isotopic substitution, matrix isolation infrared spectroscopy, combined with density functional theory (DFT) calculation, is very powerful in investigating the spectrum, structure, and bonding of novel species and the related reaction mechanisms.[19,20] Complexes such as FeN, NFeN, $(Fe_2)(N_2)$, side-on $Fe(N_2)$, and end-on Fe(NN) have been characterized from isotopic shifts and splitting patterns in the excess argon and nitrogen.[11] Recently, the binary iron−dinitrogen complex $Fe(NN)_5$ has been synthesized by codepositing mass-selected Fe cations with N_2 and electrons and identified by comparing the recorded FTIR spectrum with the results of DFT calculations.[12] To further understand the bonding nature of iron with dinitrogen, we investigated the structures, ground electronic states, and bonding characteristics of iron dinitrogen complexes by probing the N−N vibration[21] in reaction products with IR spectroscopy and DFT calculations. IR spectroscopy and theoretical calculations provide evidence for the formations of $Fe(N_2)$, $Fe(NN)_x$ ($x = 1-5$), and $Fe(NN)_3^-$. As compared to the previous reports on the reactions of Fe atoms with a high concentration of N_2 in solid argon or N_2[10−12] and considering that solid neon may stabilize some species difficult to be observed in solid argon,[4,19] we use a neon matrix to study the reactions of Fe with a lower concentration of N_2, which provides clean IR spectra and new information on $Fe(N_2)$ and $Fe(NN)_x$ ($x = 1-5$) complexes. New species of the $Fe(NN)_3^-$ anion have been obtained through the capture of an ablated electron.

Experimental and Theoretical Methods

The experiments for laser ablation and matrix isolation infrared spectroscopy are similar to those previously reported.[22] In short, the Nd:YAG laser fundamental (1064 nm, 10 Hz repetition rate with 10 ns pulse width) was focused on the rotating Fe target. The laser-ablated iron atoms were codeposited with N_2 (99.95%, Suzuki Shokan Co., Ltd.) in excess neon onto a CsI window cooled normally to 4 K by means of a closed-cycle helium refrigerator. Typically, 10−20 mJ/pulse laser power was used. Isotopic $^{15}N_2$ (99.8%, Shoko Co., Ltd.) and $^{14}N_2 + {}^{15}N_2$ mixtures were used in different experiments. In general, matrix samples were deposited for 30−60 min with a typical rate of 2−4 mmol/h. After sample deposition, IR spectra were recorded on a BIO-RAD FTS-6000e spectrometer at 0.5 cm^{-1} resolution using a liquid nitrogen cooled HgCdTe (MCT) detector for the spectral range of 5000−450 cm^{-1}. Samples were annealed at different temperatures and subjected to broad band irradiation ($\lambda > 250$ nm) using a high-pressure mercury arc lamp (Ushio, 100 W).

DFT calculations were performed to predict the structures and vibrational frequencies of the observed reaction products using the Gaussian 03 program.[23] The BP86 and B3LYP density functional methods were utilized.[24] The TZVP basis set was

* To whom correspondence should be addressed, q.xu@aist.go.jp.
[†] National Institute of Advanced Industrial Science and Technology (AIST).
[‡] Kobe University.

10.1021/jp9106298
Published on Web 01/20/2010

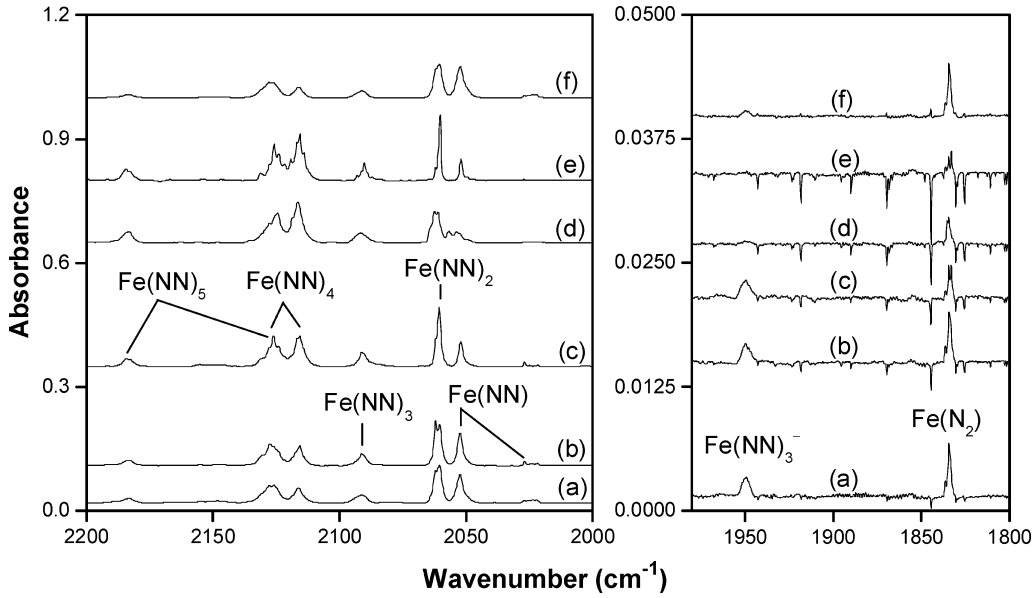

Figure 1. Infrared spectra in the 2200−2000 and 1950−1800 cm^{-1} regions from codeposition of laser-ablated Fe atoms with 0.3% N_2 in Ne at 4 K. (a) Spectrum obtained from initial deposited sample for 40 min, (b) spectrum after annealing to 8 K, (c) spectrum after annealing to 10 K, (d) spectrum after 10 min of broadband irradiation, (e) spectrum after annealing to 12 K, and (f) spectrum obtained from initially depositing laser-ablated Fe atoms with 0.3% N_2 + 0.03% CCl_4 in Ne at 4 K for 40 min.

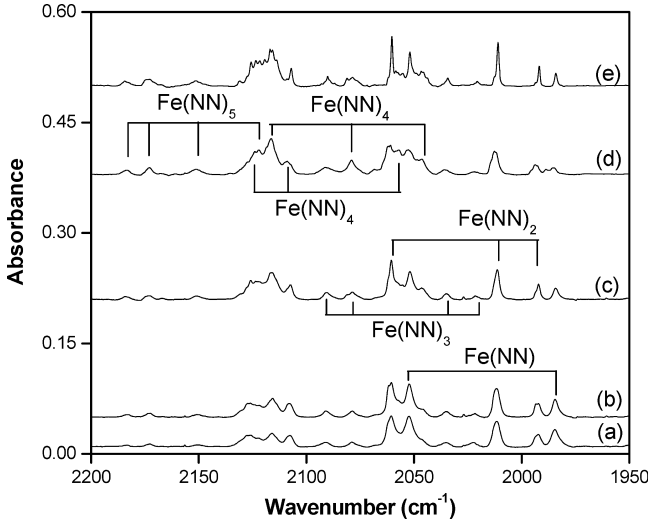

Figure 2. Infrared spectra in the 2200−1950 cm^{-1} region from codeposition of laser-ablated Fe atoms with 0.2% $^{14}N_2$ + 0.2% $^{15}N_2$ in Ne at 4 K. For the meaning of (a−e), see Figure 1.

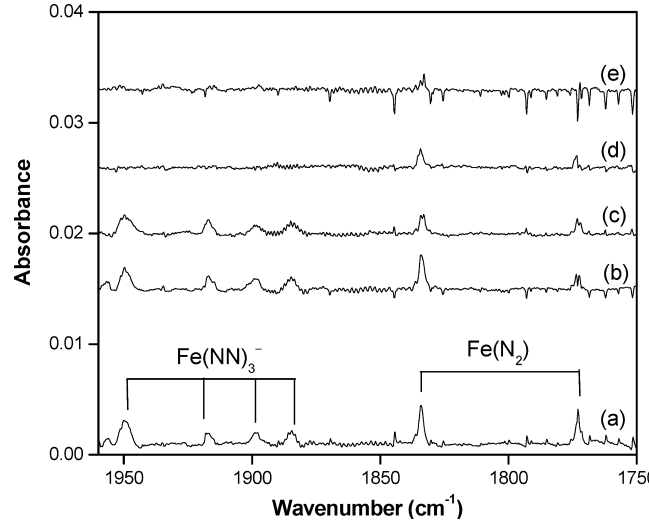

Figure 3. Infrared spectra in the 1950−1750 cm^{-1} region from codeposition of laser-ablated Fe atoms with 0.2% $^{14}N_2$ + 0.2% $^{15}N_2$ in Ne at 4 K. For the meaning of (a−e), see Figure 1.

used for the N atoms, and the DZVP basis set was used for the Fe atoms.[25] All geometrical parameters were fully optimized, and the harmonic vibrational frequencies were calculated with analytical second derivatives. A natural bond orbital (NBO)[26] approach was employed to elucidate the electron configuration and bonding characteristics. Trial calculations and recent investigations have shown that such computational methods can provide reliable information for metal complexes, such as infrared frequencies, relative absorption intensities, and isotopic shifts.[19−21]

TABLE 1: IR Absorptions (in cm^{-1}) Observed from Reaction of Laser-Ablated Fe Atoms with N_2 in Excess Neon

$^{14}N_2$	$^{15}N_2$	$^{14}N_2$ + $^{15}N_2$	$^{14}N_2/^{15}N_2$	assignment
2184.2	2111.7	2184.1, 2172.8, 2151.3, 2111.7	1.0343	$Fe(NN)_5$
2126.2	2055.4	2126.1, 2107.5, 2055.4	1.0344	$Fe(NN)_{4,5}$
2115.9	2045.8	2115.9, 2078.7, 2046.0	1.0343	$Fe(NN)_4$
2091.0	2021.4	2090.9, 2078.7, 2035.1, 2021.7	1.0344	$Fe(NN)_3$
2060.8	1992.3	2060.7, 2011.4, 1992.3	1.0344	$Fe(NN)_2$
2051.2	1984.2	2052.0, 1984.3	1.0338	Fe(NN)
2027.0	1960.7	2027.0, 1960.7	1.0338	Fe(NN) site
1949.3	1885.2	1949.3, 1918.1, 1898.5, 1884.7	1.0340	$Fe(NN)_3^-$
1834.2	1773.3	1834.1, 1772.9	1.0343	$Fe(N_2)$

Results and Discussion

Experiments have been done for laser-ablated Fe atoms reactions with N_2 in excess neon using low laser energy with different N_2 concentrations. Typical infrared spectra for the products in the selected regions are illustrated in Figures. 1−3, and the absorption bands in different isotopic experiments are listed in Table 1. These bands are observed in lower laser power experiments and not favored with higher laser energy and low N_2 concentration, suggesting that one iron atom is involved. The stepwise annealing and photolysis behavior of the product absorptions is also shown in the figures and will be discussed below.

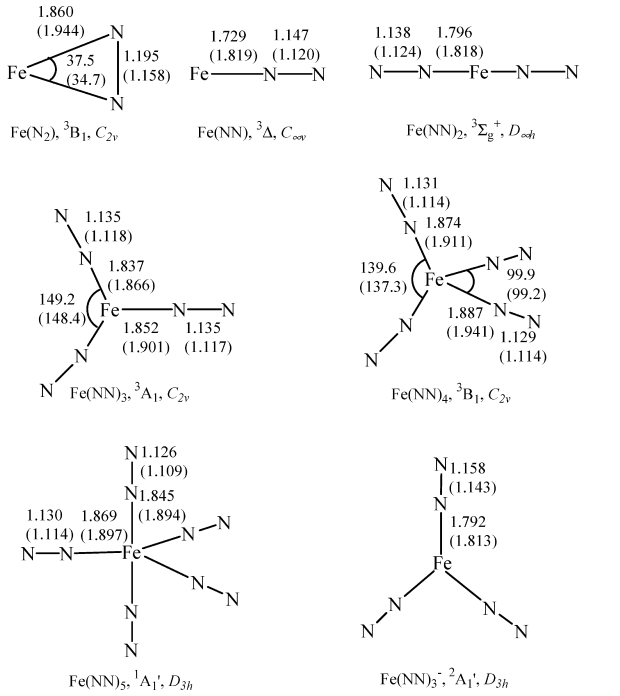

Figure 4. Optimized structures (bond lengths in angstroms, bond angles in degrees) of the $Fe(N_2)$, $Fe(NN)_x$ ($x = 1-5$), and $Fe(NN)_3^-$ complexes calculated at the BP86/6-311+G(d)-LANL2DZ and B3LYP/6-311+G(d)-LANL2DZ (in parentheses) levels.

Density functional theory calculations have been carried out for the possible isomers and electronic states of the potential product molecules. Figure 4 shows the ground state structures of the products calculated at the BP86/6-311+G(d)-LANL2DZ and B3LYP/6-311+G(d)-LANL2DZ levels. The results calculated with the B3LYP functional are in good agreement with those from BP86 calculations. Table 2 reports a comparison of the observed and calculated isotopic frequency ratios for the N−N stretching modes of the observed products. It can be found from Table 2 that the BP86 functional gives calculated N−N stretching vibrational frequencies (unscaled) much closer to the experimental values than the B3LYP functional, consistent with the previous theoretical calculations.[27] Hereafter, mainly BP86 results are presented for discussion. Ground electronic states, point groups, vibrational frequencies, and intensities are listed in Table 3. The summary of electronic configurations, natural charge distributions, and bond orders for the $Fe(NN)_x$ ($x = 1-5$) complexes are given in Table 4. Molecular orbital depictions of the highest occupied molecular orbitals (HOMOs) and HOMO-1s of the products are representatively illustrated in Figure 5.

$Fe(N_2)$. The absorption at 1834.2 cm^{-1} appears after sample deposition, increases after sample annealing, and slightly decreases after further annealing and broad band irradiation (Table 1 and Figure 1). The $^{15}N_2$ counterpart at 1773.3 cm^{-1} gives the isotopic ratio of 1.0343, which is characteristic of a N−N stretching vibration. The $^{14}N_2 + {}^{15}N_2$ experiment reveals a clear 1834.1 and 1772.9 cm^{-1} mixed isotopic doublet (Figure 3); hence, one NN subunit is involved in these vibrations. Doping with CCl_4 has no effect on the band, which suggests that the product is neutral. The isotopic $^{14}N_2/^{15}N_2$ ratio 1.0343 is slightly higher than the ratio 1.0338 for Fe(NN), which suggests more nitrogen participation in the vibrational mode owing to stronger Fe−N bonds in the side-on complex as compared to the end-on complex Fe(NN) (vide infra). Accordingly, this band is assigned to the N−N stretching vibration of the neutral side-on $Fe(N_2)$ complex, which is about 7.6 cm^{-1} blue-shifted from the corresponding absorption in an argon matrix.[11]

The BP86 calculations predict the side-on $Fe(N_2)$ complex to have a $^3B_1$ ground state with C_{2v} symmetry (Table 3 and Figure 4), which lies 3.4 kcal/mol higher in energy than the end-on Fe(NN) isomer (Figure 4). The present calculations are in good agreement with the previous DFT frequency calculations.[11,17] Briefly, the N−N stretching vibration frequency of $Fe(N_2)$ is calculated at 1728.1 cm^{-1} (Table 3). As listed in Table 2, the calculated $^{14}N_2/^{15}N_2$ isotopic frequency ratio (1.0349) is also consistent with the experimental observation (1.0343). The assignment is strongly supported by the DFT calculations.

The dissociation of N_2 is the rate-limiting step in the important Haber process for the catalytic synthesis of ammonia.[2] Molecularly adsorbed N_2 on Fe(111) has been characterized as a side-on type π-bonded surface complex in which both nitrogen atoms interact with the metal, which has been proposed as an intermediate in the catalytic dissociation of N_2.[5] The N−N frequency has been measured by high-resolution electron-energy-loss spectroscopy and was found to be 1555 cm^{-1} at 110 K. The ν_{N-N} values of the end-on species $Fe(NN)_{1-5}$ as observed in the present work (vide infra) are about 500 cm^{-1} higher than that of N_2 on Fe(111), while the 1834.2 cm^{-1} neon matrix frequency for the side-on $Fe(N_2)$ molecule may be compared with the 1555 cm^{-1} fundamental for N_2 adsorbed on Fe(111).

Fe(NN). The band at 2051.2 cm^{-1} with a trapping site at 2027.0 cm^{-1} appears after sample deposition, increases after sample annealing, visibly decreases after broad band irradiation, and recovers after further annealing to higher temperature (Table 1 and Figure 1). It shifts to 1984.2 cm^{-1} with $^{15}N_2$, giving a 1.0338 $^{14}N/^{15}N$ isotopic frequency ratio, which is characteristic of a N−N stretching vibration. The $^{14}N_2 + {}^{15}N_2$ experiment reveals a clear 2052.0 and 1984.3 cm^{-1} mixed isotopic doublet (Figure 2); hence, one NN subunit is involved in these vibrations.[29] Doping with CCl_4 has no effect on the band, which suggests that the product is neutral. Accordingly, this band is assigned to the N−N stretching vibration of the neutral Fe(NN) complex, which is about 31 cm^{-1} blue-shifted from the corresponding absorption in an argon matrix[9] and about 33 cm^{-1} blue-shifted from the corresponding absorption in a pure dinitrogen matrix.[11] It is noted that early krypton experiments tentatively assigned the absorption of Fe(NN) at 2002 cm^{-1}.[10]

A LCGTO-KS-DF calculation predicted the ground state of Fe(NN) as quintet ground state, and the triplet state lies 2.4 kcal/mol higher in energy.[14] N_2 is isoelectronic with CO. The previous BP86 and B3LYP calculations predicted a $^3\Sigma^-$ ground state with linear geometry for Fe(CO).[28] The present BP86 calculations predict Fe(NN) to have a $^3\Delta$ ground state with a linear geometry (Figure 4), which are in good agreement with the previous calculations by the DGauss program.[11] The N−N stretching vibration frequency of Fe(NN) is calculated at 2021.2 cm^{-1} (Table 3), which is in accord with our observed value of 2051.2 cm^{-1} (Table 2). As listed in Table 2, the calculated $^{14}N/^{15}N$ isotopic frequency ratio (1.0350) is also consistent with the experimental observation (1.0338). The assignment of the Fe(NN) molecule is supported by the agreement between the experimental and the calculated vibrational frequencies and isotopic shifts.

$Fe(NN)_2$. The absorption at 2060.8 cm^{-1} appears after sample deposition, increases after sample annealing, decreases after broad band irradiation, and recovers after further annealing to higher temperature (Table 1 and Figure 1). The band shifts to

TABLE 2: Comparison of Observed and Calculated IR Frequencies (in cm^{-1}) and Isotopic Frequency Ratios for the Products

	observed		BP86		B3LYP	
species	ν_{N-N}	$^{14}N_2/^{15}N_2$	ν_{N-N}	$^{14}N_2/^{15}N_2$	ν_{N-N}	$^{14}N_2/^{15}N_2$
$Fe(N_2)$	1834.2	1.0343	1728.1	1.0349	1918.4	1.0350
Fe(NN)	2051.2	1.0338	2021.2	1.0350	2209.9	1.0350
$Fe(NN)_2$	2060.8	1.0344	2059.0	1.0350	2136.8	1.0350
$Fe(NN)_3$	2091.0	1.0344	2083.1	1.0350	2193.2	1.0350
$Fe(NN)_4$	2126.2	1.0344	2123.1	1.0350	2234.6	1.0350
	2115.9	1.0343	2112.6	1.0350	2226.3	1.0350
$Fe(NN)_5$	2184.2	1.0343	2157.2	1.0350	2297.4	1.0350
	2126.2	1.0344	2130.5	1.0350	2241.8	1.0350
$Fe(NN)_3^-$	1949.3	1.0340	1940.9	1.0350	1993.3	1.0350

TABLE 3: Ground Electronic States, Point Groups, Vibrational Frequencies (in cm^{-1}), and Intensities (km/mol) of Reaction Products Calculated at the BP86/6-311+G(d)-LANL2DZ Level

species	electronic state	point group	frequency (intensity, mode)
$Fe(N_2)$	$^3B_1$	C_{2v}	1728.1 (229, A_1), 493.3 (24, A_1), 443.5 (25, B_2)
Fe(NN)	$^3\Delta$	$C_{\infty v}$	2021.2 (971, σ), 534.3 (51, σ), 289.9 (3, π), 253.2 (3, π)
$Fe(NN)_2$	$^3\Sigma_g^+$	$D_{\infty h}$	2119.6 (0, σ_g), 2059.0 (1636, σ_u), 534.8 (131, σ_u), 467.4 (2, π_u), 430.9 (0, π_u), 376.3 (11, σ_g), 260.2 (0, π_g), 257.6 (0, π_g), 67.0 (2, π_u), 44.0 (4, π_u)
$Fe(NN)_3$	$^3A_1$	C_{2v}	2154.7 (4, A_1), 2083.5 (782, A_1), 2083.1 (1300, A_1), 484.6 (90, B_2), 436.6 (0.4, A_1), 418.3 (40, A_1), 405.3 (2, B_1), 383.1 (2, A_1), 361.1 (8, B_2), 264.2 (0, B_2), 228.3 (0, A_2), 209.6 (0.4, B_1), 73.9 (1, B_2), 67.0 (1, A_1), 63.7 (3, B_1)
$Fe(NN)_4$	$^3B_1$	C_{2v}	2191.1 (11, A_1), 2123.1 (686, B_1), 2114.7 (616, A_1), 2112.6 (1075, B_1), 441.3 (65, B_2), 401.4 (5, A_1), 388.8 (12, A_1), 388.6 (6, B_1), 372.5 (38, B_1), 364.6 (18, A_1), 350.5 (0, A_2), 344.8 (3, A_1), 330.8 (17, B_2), 238.1 (0, A_2), 236.6 (0, B_2), 230.5 (0.3, B_1), 75.9 (1, B_2), 74.6 (1, A_1), 72.9 (1, B_1), 65.6 (0, A_2), 53.2 (0.1, A_1)
$Fe(NN)_5$	$^1A_1'$	D_{3h}	2218.4 (0, A_1'), 2157.2 (745, A_2'), 2137.3 (0, A_1'), 2130.5 (724 × 2, E′), 536.3 (52 × 2, E′), 488.3 (97, A_2''), 441.2 (0 × 2, E′), 410.4 (6 × 2, E), 402.5 (6, A_2''), 386.1 (0, A_1'), 362.5 (0, A_1'), 331.5 (29, E′), 280.4 (0, A_2'), 273.8 (0 × 2, E″), 105.1 (0.2 × 2, E), 97.9 (1, A_2'), 93.2 (0 × 2, E″), 51.3 (0.01 × 2, E′)
$Fe(NN)_3^-$	$^2A_1'$	D_{3h}	2028.3 (0, A_1'), 1940.9 (1724 × 2, E′), 521.4 (78 × 2, E′), 506.6 (0.1, A_2''), 489.6 (19 × 2, E′), 437.6 (0, A_1'), 308.6 (0, A_2'), 225.5 (0 × 2, E″), 69.9 (9, A_2''), 63.2 (0.3 × 2, E′)

TABLE 4: Electronic Configurations, Natural Charge Distributions, and Bond Order for $Fe(NN)_x$ ($x = 1-5$) Calculated at the BP86/6-311+G(d)-LANL2DZ Level

		natural charge[a]			bond order	
species	Fe electronic configuration	Fe	N1	N2	Fe−N1	N1−N2
Fe(NN)	$4S^{0.82}3d^{6.85}$	0.312	–0.231	–0.081	0.810	2.507
$Fe(NN)_2$	$4S^{0.57}3d^{6.95}$	0.476	–0.222	–0.016	0.615	2.609
$Fe(NN)_3$	$4S^{0.31}3d^{6.97}$	0.700	–0.224	–0.002	0.527	2.645
$Fe(NN)_4$	$4S^{0.28}3d^{6.96}$	0.712	–0.192	0.018	0.465	2.697
$Fe(NN)_5$	$4S^{0.29}3d^{7.10}$	0.545	–0.085	–0.038	0.598	2.710

[a] N1 is the nearest neighbor of Fe and N2 is the atom bonded to N1.

1992.3 cm^{-1} with $^{15}N_2$, exhibiting isotopic frequency ratio ($^{14}N_2/^{15}N_2$ 1.0344) characteristic of the N−N stretching vibration. A triplet isotopic pattern is observed in the mixed $^{14}N_2 + ^{15}N_2$ isotopic spectra (Figure 2), which indicates that two N_2 units are involved in the complex.[29] Doping with CCl_4 has no effect on the band, which suggests that the product is neutral. Accordingly, the absorption at 2060.8 cm^{-1} is assigned to the asymmetric N−N stretching mode of $Fe(NN)_2$. This assignment confirms the previous tentative assignment in solid argon (2045 cm^{-1}).[11] The N−N stretching mode for $Fe(NN)_2$ in the neon matrix is blue-shifted 15.8 cm^{-1} relative to previous argon matrix experiments.[11]

The $Fe(NN)_2$ species is predicted to have a $^3\Sigma_g^+$ ground state with $D_{\infty h}$ symmetry (Table 3 and Figure 4), consistent with the previous LCGTO-KS-DF studies.[14] The N−N asymmetric stretching mode for this linear complex is predicted at 2059.0 cm^{-1}, only 1.8 cm^{-1} lower than the neon matrix value. The calculated $^{14}N/^{15}N$ isotopic frequency ratio (1.0350) of the asymmetric N−N stretching vibration is consistent with the experimental value (1.0344). These agreements support the identification of the $Fe(NN)_2$ complex.

$Fe(NN)_3$. The absorption at 2091.0 cm^{-1} appears after sample deposition, increases after sample annealing, slightly decreases after broad band irradiation, and recovers after further annealing to higher temperature (Table 1 and Figure 1). It shifts to 2021.4 cm^{-1} with $^{15}N_2$, giving an isotopic $^{14}N/^{15}N$ ratio of 1.0344, which is characteristic of a N−N stretching vibration. In the $^{14}N_2 + ^{15}N_2$ experiment, a quartet mixed isotopic pattern (2090.9/2078.7/2035.1/2021.7) has been observed (Figure 2), which is reminiscent of the $Rh(NN)_3$ complex.[30] Doping with CCl_4 has no effect on the band, which suggests that the product is neutral. Accordingly, this band is suitable for the N−N stretching vibration of the $Fe(NN)_3$ complex. Note that the band at 2032 cm^{-1} was tentatively assigned to $Fe(NN)_3$ in the early solid krypton experiments.[10]

The previous demon-KS calculations predicted the triple state with C_{2v} geometry to be the ground state for $Fe(NN)_3$.[14] The present BP86 calculations predict that the $Fe(NN)_3$ complex has a $^3A_1$ ground state with C_{2v} symmetry (Table 3 and Figure 4) and three N−N stretching modes are calculated at 2154.7 cm^{-1} (4 km/mol, A_1), 2083.5 cm^{-1} (782 km/mol, A_1), and 2083.1 cm^{-1} (1300 km/mol, A_1). The band 2154.7 cm^{-1} with very low intensity (4 km/mol) is not readily observed and the band 2083.5 cm^{-1} couples with 2083.1 cm^{-1} in the IR spectra, which is in accord with experimental observations. As listed in Table 2, the calculated $^{14}N_2/^{15}N_2$ isotopic frequency ratio is consistent with the experimental value. The assignment of the $Fe(NN)_3$ molecule is supported by the overall agreement between the

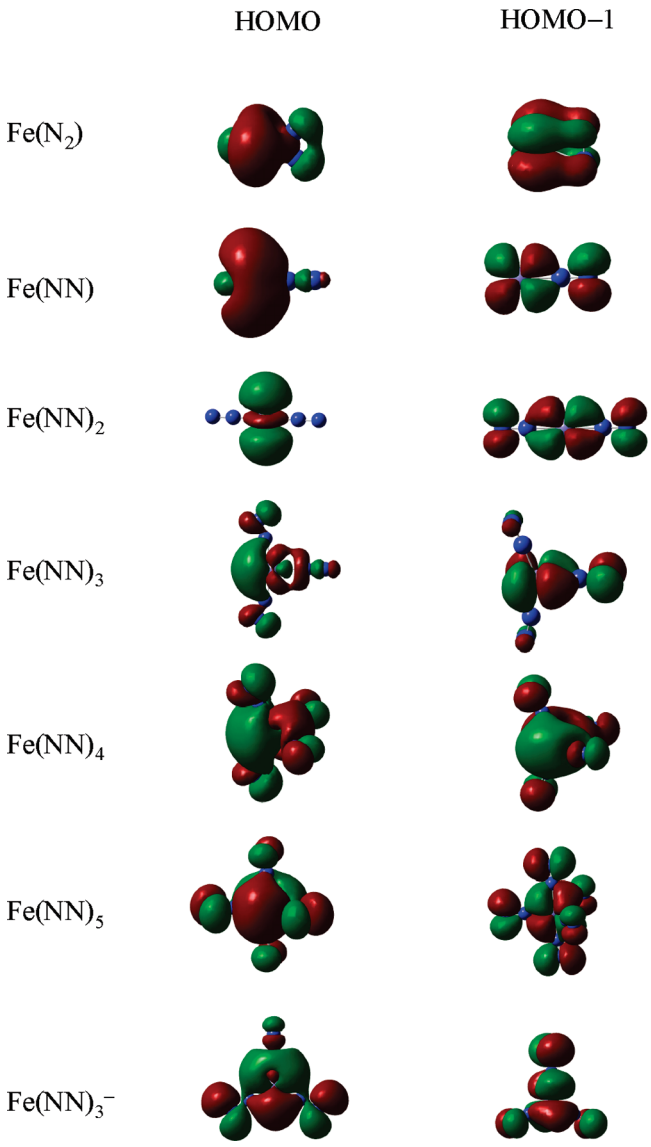

Figure 5. Molecular orbital depictions of the highest occupied molecular orbitals (HOMOs) and HOMO-1s of the $Fe(N_2)$, $Fe(NN)_x$ ($x = 1-5$), and $Fe(NN)_3^-$ complexes calculated at the BP86/6-311+G(d)-LANL2DZ level.

experimental and the calculated vibrational frequencies, isotopic shifts, and relative intensities.

$Fe(NN)_4$. The absorptions at 2126.2 and 2115.9 cm^{-1} appear together after sample deposition and increase after sample annealing and broad band irradiation (Table 1 and Figure 1). The two bands shift to 2055.4 and 2045.8 cm^{-1} with $^{15}N_2$, respectively, giving isotopic frequency ratios ($^{14}N/^{15}N$, 1.0344 and 1.0343) characteristic of N−N stretching vibrations. Two different triplet isotopic patterns are observed in the mixed $^{14}N_2 + {}^{15}N_2$ isotopic spectra (Figure 2, trace d), which indicate that four N_2 units are involved in the complex.[29] Doping with CCl_4 has no effect on these bands, suggesting that the product is neutral. As compared with the DFT calculations (vide infra), the absorptions at 2126.2 and 2115.9 cm^{-1} can be assigned to the asymmetric N−N stretching modes of the $Fe(NN)_4$ complex. It is noted that in the previous solid krypton, the bands at 2086, 2098, and 2108 cm^{-1} were tentatively assigned to $Fe(NN)_4$.[10]

The $Fe(NN)_4$ complex is predicted to have a $^3B_1$ ground state with C_{2v} symmetry (Table 3 and Figure 4), in accord with the previous deMon-KS studies.[14] The N−N stretching frequencies of the $Fe(NN)_4$ species are calculated to be 2191.1 (11 km/mol, A_1), 2123.1 (686 km/mol, B_1), 2114.7 (616 km/mol, A_1), and 2112.6 (1075 km/mol, B_1) cm^{-1}, respectively. The 2191.1 cm^{-1} band with very low intensity (11 km/mol) is not readily to be observed, which is in line with the absence of this mode of the $Fe(NN)_4$ complex from the present experiments. The band 2112.6 cm^{-1} couples with 2114.7 cm^{-1} in the IR spectra, consistent with the observed frequency of 2115.9 cm^{-1}. In addition, the calculated band 2123.1 cm^{-1} is only 3.1 cm^{-1} lower than the neon matrix value 2126.2 cm^{-1}. All other modes of $Fe(NN)_4$ with IR intensities less than 70 km/mol (Table 3) are not readily observed, which are in line with the absence of these modes of the $Fe(NN)_4$ complex from the present experiments. Furthermore, the calculated $^{14}N/^{15}N$ isotopic frequency ratios of the N−N stretching vibrations are also in accord with the experimental values (Table 2), which supports the identification of the $Fe(NN)_4$ complex.

$Fe(NN)_5$. The absorptions at 2184.2 and 2126.2 cm^{-1} appear on sample deposition and increase after sample annealing and broad band irradiation (Table 1 and Figure 1). These two bands shift to 2111.7 and 2055.4 cm^{-1} with $^{15}N_2$, exhibiting isotopic frequency ratios ($^{14}N/^{15}N$, 1.0343 and 1.0344) characteristic of N−N stretching vibrations. As can be seen in Table 1 and Figure 2, a quartet isotopic pattern (2184.1/2172.8/2151.3/2111.7) and a triple isotopic pattern (2126.1/2107.5/2055.4) have been observed in the mixed $^{14}N_2 + {}^{15}N_2$ experiments. Doping with CCl_4 has no effect on the bands, which suggests that the product is neutral. By comparing the IR spectra with the results of DFT calculations (vide infra), these two bands are suitable for the N−N stretching modes of the $Fe(NN)_5$ complex. In the previous experiments in solid nitrogen, the bands at 2012 and 2106 cm^{-1} were tentatively assigned to $Fe(NN)_5$ with D_{3h} symmetry.[10] In recent N_2 matrix experiments, three peaks at 2071, 2078, and 2095 cm^{-1} were attributed to the D_{3h} end-on $Fe(N_2)_5$ complex.[12]

BP86 calculations predict $Fe(NN)_5$ to have a $^1A_1'$ ground state with D_{3h} symmetry (Table 3 and Figure 4), which is in line with the previous LCGTO-KS-DF calculations.[12,14] As listed in Table 3, the asymmetric N−N stretching vibration frequencies of $Fe(NN)_5$ are calculated to be 2157.2 and 2130.5 cm^{-1}, consistent with the neon matrix observation at 2184.2 and 2126.2 cm^{-1}. The calculated $^{14}N/^{15}N$ isotopic frequency ratios (1.0350 and 1.0349) are also consistent with the experimental values (1.0338 and 1.0343). In addition, all other modes of $Fe(NN)_5$ with low IR intensities (Table 3) are not readily observed, which are consistent with the absence of these modes of the $Fe(NN)_5$ complex from the present experiments. These agreements between the experimental and the calculated results support the assignment of the $Fe(NN)_5$ complex.

$Fe(NN)_3^-$. The absorption at 1949.3 cm^{-1} appears after sample deposition, increases after sample annealing, disappears after broad band irradiation, and does not recover after further annealing to higher temperature (Table 1 and Figure 1). It shifts to 1885.2 cm^{-1} with $^{15}N_2$, giving an isotopic $^{14}N/^{15}N$ ratio of 1.0340, which is characteristic of a N−N stretching vibration. The approximately 2:1:1:2 isotopic distribution is obtained in $^{14}N_2 + {}^{15}N_2$ experiments (Figure 3), indicating that three equivalent NN subunits are involved in this molecule.[29] Doping with CCl_4 in the N_2/Ne sample with 1/10 concentration of N_2 eliminates this band, suggesting an anionic species identification. Accordingly, this band is assigned to the N−N stretching vibration of the $Fe(NN)_3^-$ anion.

The $Fe(NN)_3^-$ complex is predicted to have a $^2A_1'$ ground state with D_{3h} symmetry (Table 3 and Figure 4). A strong asymmetric mode at 1940.9 cm^{-1} is predicted for $Fe(NN)_3^-$, which is only about 8.4 cm^{-1} lower than the neon matrix value.

The calculated $^{14}N/^{15}N$ isotopic frequency ratio (1.0350) of the asymmetric N−N stretching vibration is consistent with the experimental value (1.0340), which confirms the identification of the $Fe(NN)_3^-$ anion.

Bonding Consideration. It is interesting to compare the electronic configurations, natural charge distributions, and bond orders for the $Fe(NN)_x$ ($x = 1-5$) complexes in Table 4. The ground-state electronic configuration of the Fe atom is $4s^23d^6$. In the $Fe(NN)_x$ ($x = 1-5$) complexes; however, the NBO analyses reveal that there are some electrons (0.85−1.1 electrons) transferred from 4s to 3d, implying the strong hybridization between 4s and 3d of the Fe atom. The removal of 4s electrons of Fe reduces the Fe−N σ repulsion and enhances the Fe to N_2 π^* back-donation. The natural charge distribution on Fe(NN) shows a transfer of about 0.312 electron from Fe to NN. The N−N bond weakens due to the π back-donation, and the N−N bond in Fe(NN) is elongated 0.036 Å from free N_2, and consequently, the N−N stretching frequency for Fe(NN) is red-shifted 303.5 cm^{-1} from free N_2. The change of natural charge can be taken as a measure of the π back-donation. As the number of NN ligands increases, the natural charge on the N1 and N2 atoms decreases monotonically (N1 is the nearest neighbor of the Fe atom whereas N2 is the atom bonded to N1), suggesting that the π back-donation diminishes from one NN ligand to five ligands. When five NN ligands are placed around the Fe atom, the electron transfer from Fe to N1 and N2 via π back-donation is not efficient, so that the natural charge on N1 and N2 is markedly decreased in $Fe(NN)_5$. As can be seen from the bond orders of Fe−N1 and N1−N2 in Table 4, the Fe−N bond is weakened whereas the N−N bond is enhanced upon the increase of NN ligands. Therefore, the N−N stretching vibrations increase with increasing NN ligands, in agreement with experimental observations (Table 1).

As illustrated in Figure 5, the highest occupied molecular orbital (HOMO) in the linear Fe(NN) is of σ-type with the contribution mainly from the Fe 3d and N 2p atomic orbitals, whereas the HOMO in the linear $Fe(NN)_2$ is largely Fe 4s and 3d in character and is nonbonding. The HOMO-1s in Fe(NN) and $Fe(NN)_2$ are degenerate of π-type and mainly result from the contributions between the Fe 3d and N 2p atomic orbitals. The HOMO in the side-on $Fe(N_2)$ is a σ-type bond whereas the HOMO-1 is a δ-type bond. As can be seen from the HOMO in the side-on $Fe(N_2)$ complex with the acute NFeN angle, the nitrogen atoms are close enough in proximity to produce a significant N−N bonding interaction, which facilitates the back-donation from the Fe atom to the N_2 ligand. For the $Fe(NN)_x$ ($x = 3-5$) and $Fe(NN)_3^-$ complexs, the HOMOs are of σ-type whereas the HOMO-1s are of π-type, which are responsible for the stability of these metal dinitrogen complexes.

Reaction Pathways. In our experiments, no IR absorptions due to nitrides were observed in the as-deposited and annealed spectra, suggesting that in the present experiments, the laser ablation conditions were not significant for generating Fe atoms with energies high enough to dissociate molecular N_2 to N atoms, indicating that the observed products were formed by low-temperature reactions of the Fe atoms with molecular N_2. On the basis of the behavior of sample annealing and irradiation, together with the observed species and calculated stable isomers, plausible reaction pathways can be proposed as follows. Laser-ablated Fe atoms are codeposited with N_2 to form the $Fe(N_2)$, $Fe(NN)_x$ ($x = 1-5$), and $Fe(NN)_3^-$ complexes (Figure 1). The absorptions of iron dinitrogen complexes increase on annealing, suggesting the reactions to form these species are spontaneous. The iron dinitrogen complexes may be formed from the reactions of Fe atoms or iron dinitrogen complexes with N_2 (reactions 1−7). As can be seen in reactions 1−7, all association reactions are predicted to be exothermic (−7.5 to −43.4 kcal/mol), in agreement with the experimental observations.

Recent investigations have shown that laser ablation of metal targets produces not only neutral metal atoms but also metal cations and electrons, and ionic metal complexes can also be formed in the reactions with small molecules.[31,32] In the present experiments, the $Fe(NN)_3^-$ anion appears during sample deposition and changes little after sample annealing and other anions absent, suggesting the species may be generated through the capture of ablated electron at the expense of $Fe(NN)_3$ (reaction 7).

$$Fe(^5D) + N_2(^1\Sigma_g^+) \rightarrow Fe(N_2)(^3B_1) \quad (1)$$

$$\Delta E = -9.5 \text{ kcal/mol}$$

$$Fe(^5D) + N_2(^1\Sigma_g^+) \rightarrow FeNN(^3\Delta) \quad (2)$$

$$\Delta E = -12.9 \text{ kcal/mol}$$

$$FeNN(^3\Delta) + N_2(^1\Sigma_g^+) \rightarrow Fe(NN)_2(^3\Sigma_g^+) \quad (3)$$

$$\Delta E = -40.5 \text{ kcal/mol}$$

$$Fe(NN)_2(^3\Sigma_g^+) + N_2(^1\Sigma_g^+) \rightarrow Fe(NN)_3(^3A_1) \quad (4)$$

$$\Delta E = -21.4 \text{ kcal/mol}$$

$$Fe(NN)_3(^3A_1) + N_2(^1\Sigma_g^+) \rightarrow Fe(NN)_4(^3B_1) \quad (5)$$

$$\Delta E = -17.6 \text{ kcal/mol}$$

$$Fe(NN)_4(^3B_1) + N_2(^1\Sigma_g^+) \rightarrow Fe(NN)_5(^1A_1') \quad (6)$$

$$\Delta E = -7.5 \text{ kcal/mol}$$

$$Fe(NN)_3(^3A_1) + e^- \rightarrow Fe(NN)_3^-(^2A_1') \quad (7)$$

$$\Delta E = -43.4 \text{ kcal/mol}$$

Conclusions

Reactions of laser-ablated iron atoms with dinitrogen in solid neon have been investigated using matrix-isolation infrared spectroscopy. The absorptions at 1834.2, 1949.3, 2051.2, 2060.8, 2091.0, 2115.9, 2126.2, and 2184.2 cm^{-1} are assigned to the N−N stretching vibrations of the $Fe(N_2)$, $Fe(NN)_3^-$, Fe(NN), $Fe(NN)_2$, $Fe(NN)_3$, $Fe(NN)_4$, and $Fe(NN)_5$ molecules, respectively, on the basis of isotopic shifts, mixed isotopic splitting patterns, and CCl_4-doping experiments. Density functional theory calculations have been performed on these complexes. The identifications of these iron dinitrogen complexes are confirmed by the overall agreement between the experimental and calculated vibrational frequencies, relative absorption intensities, and isotopic shifts.

Acknowledgment. The authors thank the reviewers for valuable suggestions and comments. This work was supported by AIST and a Grant-in-Aid for Scientific Research (B) (Grant No. 17350012) from the Ministry of Education, Culture, Sports, Science and Technology (MEXT) of Japan. Z.-H.L. acknowledges JASSO and Kobe University for an Honors Scholarship.

References and Notes

(1) Cotton, F. A.; Wilkinson, G.; Murillo, C. A.; Bochmann, M. *Advanced Inorganic Chemistry*, 6th ed.; Wiley: New York, 1999.

(2) See for example: Ertl, G. *J. Vac. Sci. Technol., A* **1983**, *1*, 1247.

(3) (a) Samuel, D. M. *Industrial Chemistry-Inorganic*; Royal Society of London: London, 1970. (b) *A Treatise on Dinitrogen Fixation*; Hardy, R. W. F., Bottomley, F., Burns, R. C., Eds.; Wiley: New York, 1979.

(4) (a) Himmel, H. J.; Reiher, M. *Angew Chem., Int. Ed.* **2006**, *45*, 6264. (b) MacLachlan, E. A.; Fryzuk, M. D. *Organometallics* **2006**, *25*, 1530. (c) Gambarotta, S.; Scott, J *Angew Chem., Int. Ed.* **2004**, *43*, 5298. (d) MacKay, B. A.; Fryzuk, M. D. *Chem. Rev.* **2004**, *104*, 385. (e) Himmel, H. J.; Downs, A. J.; Greene, T. M. *Chem. Rev* **2002**, *102*, 4191. (f) Hidai, M.; Mizobe, Y. *Chem. Rev.* **1995**, *95*, 1115.

(5) (a) Grunze, M.; Golze, M.; Hirschwald, W.; Freund, H.-J.; Plum, H.; Seip, U.; Tsai, M. C.; Ertl, G.; Kuppers, J. *Phys. Rev. Lett.* **1984**, *53*, 850. (b) Tsai, M. C.; Seip, U.; Bassignana, I. C.; Kuppers, J.; Etrl, G. *Surf. Sci.* **1985**, *155*, 387. (c) Rao, C. N. R.; Rao, G. R. *Surf. Sci. Rep.* **1991**, *13*, 221.

(6) (a) Westerberg, S.; Wang, C.; Chou, K.; Somorjai, G. A. *J. Phys. Chem. B* **2004**, *108*, 6374. (b) Pedersen, M. ø.; österlund, L.; Mortensen, J. J.; Mavrikakis, M.; Hansen, L. B.; Stensgaard, I.; Lægagaard, E.; Nørskov, J. K.; Besenbacher, F. *Phys. Rev. Lett.* **2000**, *84*, 4898.

(7) Tan, L.; Liu, F.; Armentrout, P. B. *J. Chem. Phys.* **2006**, *124*, 084302.

(8) Ding, K.; Pierpont, A. W.; Brennessel, W. W.; Lukat-Rodgers, G.; Rodgers, K. R.; Cundari, T. R.; Bill, E.; Holland, P. L. *J. Am. Chem. Soc.* **2009**, *131*, 9471.

(9) Ozin, G. A.; VanderVoet, A. *Acc. Chem. Res.* **1973**, *6*, 313.

(10) Doeff, M. M.; Parker, S. F.; Barrett, P. H.; Pearson, R. G. *Inorg. Chem.* **1984**, *23*, 4108.

(11) Chertihin, G. V.; Andrews, L.; Neurock, M. *J. Phys. Chem.* **1996**, *100*, 14609.

(12) Haslett, T. L.; Fedrigo, S.; Bosnick, K.; Moskovits, M.; Duarte, H. A.; Salahub, D. *J. Am. Chem. Soc.* **2000**, *122*, 6309.

(13) Yamada, Y.; Shimasaki, H.; Okamura, Y.; Ono, Y.; Katsumata, K. *Appl. Radiat. Isot.* **2001**, *54*, 21.

(14) Duarte, H. A.; Salahub, D. R.; Haslett, T.; Moskovits, M. *Inorg. Chem.* **1999**, *38*, 3895.

(15) Lein, M.; Frunzke, J.; Timoshkin, A.; Frenking, G. *Chem.—Eur. J.* **2001**, *7*, 4155.

(16) Seibahn, P. E. M.; Blomberg, M. R. A. *Chem. Phys.* **1984**, *87*, 189.

(17) (a) Bauschilicher, C. W., Jr.; Petterson, L. G. M.; Seigbahn, P. E. M. *J. Chem. Phys.* **1987**, *87*, 2129. (b) Seigbahn, P. E. M. *J. Chem. Phys.* **1991**, *95*, 364.

(18) Fiedler, A.; Iwata, S. *Chem. Phys. Lett.* **1997**, *271*, 143.

(19) (a) Andrews, L.; Citra, A. *Chem. Rev.* **2002**, *102*, 885. (b) Wang, G. J.; Zhou, M. F. *Int. Rev. Phys. Chem.* **2008**, *27*, 1. (c) Li, J.; Bursten, B. E.; Liang, B.; Andrews, L. *Science* **2002**, *295*, 2242. (d) Andrews, L.; Wang, X. *Science* **2003**, *299*, 2049. (e) Zhou, M. F.; Jin, X.; Gong, Y.; Li, J. *Angew. Chem., Int. Ed.* **2007**, *46*, 2911. (f) Wang, X.; Andrews, L. *J. Am. Chem. Soc.* **2008**, *130*, 6766.

(20) (a) Zhou, M. F.; Tsumori, N.; Li, Z.; Fan, K.; Andrews, L.; Xu, Q. *J. Am. Chem. Soc.* **2002**, *124*, 12936. (b) Zhou, M. F.; Xu, Q.; Wang, Z.; Schleyer, P. v. R. *J. Am. Chem. Soc.* **2002**, *124*, 14854. (c) Jiang, L.; Xu, Q. *J. Am. Chem. Soc.* **2005**, *127*, 42. (d) Xu, Q.; Jiang, L.; Tsumori, N. *Angew. Chem., Int. Ed.* **2005**, *44*, 4338. (e) Jiang, L.; Xu, Q. *J. Phys. Chem. A* **2005**, *109*, 1026.

(21) (a) Pillai, E. D.; Jaeger, T. D.; Duncan, M. A. *J. Am. Chem. Soc.* **2007**, *129*, 2297. (b) Pillai, E. D.; Jaeger, T. D.; Duncan, M. A. *J. Phys. Chem. A* **2005**, *109*, 3521.

(22) (a) Burkholder, T. R.; Andrews, L. *J. Chem. Phys.* **1991**, *95*, 8697. (b) Hassanzadeh, P.; Andrews, L. *J. Chem. Phys.* **1992**, *96*, 9177. (c) Lu, Z. H.; Jiang, L.; Xu, Q. *J. Chem. Phys.* **2009**, *131*, 034512.

(23) Frisch, M. J.; Trucks, G. W.; Schlegel, H. B.; Scuseria, G. E.; Robb, M. A.; Cheeseman, J. R.; Montgomery, J. A., Jr.; Vreven, T.; Kudin, K. N.; Burant, J. C.; Millam, J. M.; Iyengar, S. S.; Tomasi, J.; Barone, V.; Mennucci, B.; Cossi, M.; Scalmani, G.; Rega, N.; Petersson, G. A.; Nakatsuji, H.; Hada, M.; Ehara, M.; Toyota, K.; Fukuda, R.; Hasegawa, J.; Ishida, M.; Nakajima, T.; Honda, Y.; Kitao, O.; Nakai, H.; Klene, M.; Li, X.; Knox, J. E.; Hratchian, H. P.; Cross, J. B.; Adamo, C.; Jaramillo, J.; Gomperts, R.; Stratmann, R. E.; Yazyev, O.; Austin, A. J.; Cammi, R.; Pomelli, C.; Ochterski, J. W.; Ayala, P. Y.; Morokuma, K.; Voth, G. A.; Salvador, P.; Dannenberg, J. J.; Zakrzewski, V. G.; Dapprich, S.; Daniels, A. D.; Strain, M. C.; Farkas, O.; Malick, D. K.; Rabuck, A. D.; Raghavachari, K.; Foresman, J. B.; Ortiz, J. V.; Cui, Q.; Baboul, A. G.; Clifford, S.; Cioslowski, J.; Stefanov, B. B.; Liu, G.; Liashenko, A.; Piskorz, P.; Komaromi, I.; Martin, R. L.; Fox, D. J.; Keith, T.; Al-Laham, M. A.; Peng, C. Y.; Nanayakkara, A.; Challacombe, M.; Gill, P. M. W.; Johnson, B.; Chen, W.; Wong, M. W.; Gonzalez, C.; Pople, J. A. *Gaussian 03, revision B.04*; Gaussian, Inc.: Pittsburgh, PA, 2003.

(24) (a) Perdew, J. P. *Phys. Rev. B* **1986**, *33*, 8822. (b) Becke, A. D. *J. Chem. Phys.* **1993**, *98*, 5648. (c) Lee, C.; Yang, E.; Parr, R. G. *Phys. Rev. B* **1988**, *37*, 785.

(25) Godbout, N.; Salahub, D. R.; Andzelm, J.; Wimmer, E. *Can. J. Chem.* **1992**, *70*, 560.

(26) Glendening, E. D.; Reed, A. E.; Carpenter, J. E.; F. Weinhold, NBO, version 3.1, University of Wisconsin, Madison, WI, 1995.

(27) (a) Jiang, L.; Xu, Q. *J. Chem. Phys.* **2008**, *128*, 124317. (b) Feng, X.; Gu, J.; Xie, Y.; King, R. B.; Schaefer, H. F. *J. Chem. Theor. Comput* **2007**, *3*, 1580. (c) Zhao, S.; Li, Z. H.; Wang, W. N.; Liu, Z. P.; Fan, K. N.; Xie, Y.; Schaefer, H. F. *J. Chem. Phys.* **2006**, *124*, 184102.

(28) (a) Zhou, M. F.; Chertihin, G. V.; Andrews, L. *J. Phys. Chem.* **1998**, *109*, 10893. (b) Zhou, M. F.; Andrews, L. *J. Phys. Chem.* **1999**, *110*, 10370.

(29) Darling, J. H.; Ogden, J. S. *J. Chem. Soc., Dalton Trans.* **1972**, 2496.

(30) Wang, X.; Andrews, L. *J. Phys. Chem. A* **2002**, *106*, 2457.

(31) (a) Zhou, M. F.; Andrews, L.; Bauschlicher, C. W., Jr. *Chem. Rev* **2001**, *101*, 1931 references therein. (b) Gong, Y.; Zhou, M. F.; Andrews, L. *Chem. Rev.* **2009**, *109*, 6765, and references therein.

(32) (a) Zhou, M. F.; Zeng, A. H.; Wang, Y.; Kong, Q. Y.; Wang, Z. X.; Schleyert, P. V. *J. Am. Chem. Soc.* **2003**, *125*, 11512. (b) Zhou, M. F.; Zhao, Y. Y.; Gong, Y.; Li, J. *J. Am. Chem. Soc.* **2006**, *128*, 2504.

JP9106298